

Supporting Information

Nanomolar Affinity Protein *Trans*-Splicing Monitored in Real-Time by Fluorophore-Quencher Pairs

Markus Braner[†], Ralph Wieneke[†], and Robert Tampé^{*,†}

[†]Institute of Biochemistry, Biocenter, Goethe University Frankfurt,
Max-von-Laue-Str. 9, 60438 Frankfurt a. M., Germany

Table of Contents for Supporting Information

Abbreviations	3
General remarks.....	4
Molecular cloning.....	4
Protein expression and purification	5
Preparation of human cell lysates.....	5
Protein <i>trans</i> -splicing assay.....	5
Interaction analysis by microscale thermophoresis.....	5
Fluorescence dequenching analysis	6
Real-time monitoring of <i>trans</i> -splicing.....	6
Analysis of protein <i>trans</i> -splicing kinetics	6
Solid-phase peptide synthesis and Ni(II) loading	6
Tab. S1. RP-C ₁₈ HPLC gradients.....	8
Tab. S2. Calculated and observed molecular weights of synthetic I ^N fragments	8
Tab. S3. Summary of fluorescence increase, splice product formation, affinity, and kinetics..	9
Fig. S1. Chemical structures of synthetic I ^N fragments.....	10
Fig. S2. Analytical RP-C ₁₈ HPLC of synthetic I ^N fragments and MALDI-TOF MS analysis	11
Fig. S3. UV/Vis spectroscopy of F/Q-modified I ^N	12
Fig. S4. Distance estimation between fluorophore and quencher.....	13
Fig. S5. N-terminal cleavage of I ^N fragments	14
Fig. S6. Microscale thermophoresis analysis of F/Q-modified I ^N fragments with HI ^{CT}	15
Fig. S7. Fluorescence dequenching and $\tau_{1/2}$ determination of <i>trans</i> -splicing	16
Fig. S8. Fragment association investigated by fluorescence anisotropy	17
Fig. S9. Reaction kinetics of protein <i>trans</i> -splicing.....	18
Fig. S10. Real-time monitoring of protein <i>trans</i> -splicing.....	19
References.....	20

Abbreviations

aa	amino acid
BHQ-3	black hole quencher 3
Boc	<i>tert</i> -butoxycarbonyl
COMU	(1-cyano-2-ethoxy-2-oxoethylideneaminoxy)dimethylamino morpholinocarbenium hexafluorophosphate
Dap	diaminopropionic acid
DIPEA	<i>N,N</i> -diisopropylethylamine
DMEM	Dulbecco's modified eagle medium
DMF	dimethylformamide
DMSO	dimethylsulfoxide
<i>E. coli</i>	<i>Escherichia coli</i>
EDC	1-ethyl-3-(3-dimethylamino-propyl)-carbodiimide hydrochloride
EDT	1,2-ethanedithiol
EDTA	ethylenediaminetetraacetic acid
EtOAc	ethyl acetate
Et ₂ O	diethyl ether
EtOH	ethanol
ex/em	excitation/emission
FAM	5(6)-carboxyfluorescein
Fmoc	fluorenylmethoxycarbonyl
FCS	fetal calf serum
F/Q	fluorophore/quencher
HBTU	<i>O</i> -(benzotriazol-1-yl)- <i>N,N,N',N'</i> -tetramethyluronium hexafluorophosphate
HEPES	4-(2-hydroxyethyl)-1-piperazineethanesulfonic acid
His ₆	hexahistidine
HOBt*H ₂ O	hydroxybenzotriazole hydrate
HPLC	high performance liquid chromatography
IMAC	immobilized metal ion affinity chromatography
MALDI-TOF MS	matrix-assisted laser desorption/ionization – time of flight mass spectrometry
MBHA	methylbenzhydramine
MeCN	acetonitrile
MeOH	methanol
Mmt	monomethoxytrityl
MST	microscale thermophoresis
MW	molecular weight
NHS	<i>N</i> -hydroxy succinimide
NMM	<i>N</i> -methylmorpholine

NMP	<i>N</i> -methyl-2-pyrrolidon
NTA	<i>N</i> -nitrilotriacetic acid
ODS	octadecylsilane
PBS	phosphate buffered saline
RP	reverse phase
RT	room temperature
sCy5	sulfo-Cy5
S.D.	standard deviation
SDS-PAGE	sodium dodecyl sulfate polyacrylamide gel electrophoresis
SP	splice product
SPPS	solid-phase peptide synthesis
<i>t</i> Bu	<i>tert</i> -butyl
<i>t</i> BuOH	<i>tert</i> -butanol
TCEP	tris(2-carboxyethyl)-phosphine
TFA	trifluoroacetic acid
TIPS	triisopropylsilane
<i>tris</i> NTA	<i>tris-N</i> -nitrilotriacetic acid
Trx	thioredoxin

General remarks

All reagents were of the highest analytical grade, supplied by Acros Organics (Geel, Belgium), GE Healthcare (Munich, Germany), Roth (Karlsruhe, Germany), Sigma-Aldrich (Munich, Germany), or VWR (Darmstadt, Germany). Fmoc-protected amino acids and COMU were obtained from Iris Biotech (Marktredwitz, Germany) and Carbolution Chemicals (Saarbrücken, Germany). sCy5 NHS was obtained from Lumiprobe (Hannover, Germany), BHQ-3 NHS was purchased from Biosearch Technologies (Petaluma/ CA, U.S.A.), and Dabcyl NHS was ordered from TCI Chemicals (Zwijndrecht, Belgium). All assays were performed at least in triplicate and standard deviations (S.D.) were calculated.

Molecular cloning

Plasmid construction His₆-I^{C(N154A, S+1A)}-Trx. The expression plasmid encoding for HI^{C(N154A, S+1A, H73A)}T¹ was amplified with the primer pair forward (fw) 5'-GCAACAGCAAATGCTCATAGATTTTAACTATTG-3' (mutated codon in italics) and reverse (rev) 5'-GTAAAAATCTAGCATTTGCTGTTGCCTTGATAG-3' (mutated codon in italics) to perform the mutation of A73H in a whole cycle PCR. After digestion with DpnI, the resulting PCR product was ligated to yield a plasmid coding for HI^{C(N154A, S+1A, A73H)}T, thereafter referred to HI^{C(N154A, S+1A)}T.

Protein expression and purification

Protein expression in *E. coli* BL21 and IMAC purification of splice-active His₆-I^C-Trx (HI^CT), splice-inactive His₆-I^{C(N154A, S+1A, H73A)}-Trx (HI^{C(N154A, S+1A, H73A)}T), and His₆-I^{C(N154A, S+1A)}-Trx (HI^{C(N154A, S+1A)}T) or were performed as previously described.^{1,2} I^C is the C-terminal intein fragment (aa 12-154) from *Synechocystis sp.* PCC6803 DnaB (*Ssp* DnaB) M86 mini-intein. HI^{C(N154A, S+1A)}T contains two mutations at the C-terminal splice junction, which selectively allow an N-S acyl shift and potential N-terminal cleavage.

Preparation of human cell lysates

HeLa cells were grown up to 80-90% confluence in DMEM containing 10% (v/v) FCS (Gibco) under standard cell culture conditions (37 °C, 5% CO₂), harvested, and centrifuged at 120 x g (5 min, 4 °C). After washing once with PBS, centrifugation was repeated. The resulting cell pellet was dounced for 6-10 min on ice. Centrifugation at 180,000 x g for 30 min at 4 °C was then performed to remove cell membranes. The supernatant was used as a whole-cell lysates with 30 mg/mL, determined by Bradford assay.

Protein *trans*-splicing assay

All *trans*-splicing reactions were performed in splicing buffer (50 mM Tris, 300 mM NaCl, 1 μM EDTA, 0.1 mM TCEP, 10% glycerol, pH 7.0). I^N and I^C fragments were mixed at the indicated concentrations in splicing buffer and incubated for 1 h at 25 °C. For SDS-PAGE in-gel fluorescence analysis, the reaction was quenched by adding SDS loading buffer (125 mM Tris, 20% glycerol, 5% β-mercaptoethanol, 4% (w/v) SDS, 0.02% (w/v) bromophenol blue) and boiled at 95 °C for 10 min before transfer onto a reducing SDS-PAGE (12%). SDS-PAGE in-gel fluorescence was detected with an Image Quant LAS 4000 (GE Healthcare) at ex/em = 460/510 nm (FAM) and ex/em = 630/670 nm (sCy5).

Interaction analysis by microscale thermophoresis

Microscale thermophoresis was carried out by the Monolith NT.115Pico and NT.115 Nano BLUE/GREEN (NanoTemper, Munich). Splice-inactive HI^{C(N154A, S+1A, H73A)}T was serially diluted from 5000 down to 0.31 nM and 2 nM of F/Q-modified I^N fragment were added. 0.05% (v/v) Tween-20 and 50 μM EDTA were added to the buffer. Further, measurements were performed in the absence and presence of human cell lysates. The samples were incubated at 25 °C for 5-10 min before being loaded into standard treated capillaries. All samples were measured by standard protocols (70% laser intensity, 20-80% MST power, IR laser λ = 1480 nm). The normalized fluorescence F_{norm} is the parameter to quantify binding via MST by the ratio of F_{hot} (fluorescence after thermodiffusion) and F_{cold} (initial fluorescence).³

$$F_{\text{norm}} = \frac{F_{\text{hot}}}{F_{\text{cold}}} \quad (\text{Eq. 1})$$

Changes in the fluorescent thermophoresis signals were plotted against the concentration of the serially diluted I^C.

$$[AB] = \frac{[A] + [B] + K_D - \sqrt{([A] + [B] + K_D)^2 - 4[AB]}}{2[B]} \quad (\text{Eq. 2})$$

A, B: binding partner; AB: bound complex; K_D : equilibrium dissociation constant. K_D values were determined by using Eq. 2.

Fluorescence dequenching analysis

Fluorescence intensity of the F/Q-modified I^N fragments (F) was compared to the fluorescence intensity of the corresponding fluorophore-labeled I^N (F_0) to calculate the quenching efficiency (QE) according to formula:

$$QE = \frac{(F_0 - F) \cdot 100}{F_0} \quad (\text{Eq. 3})$$

As a proof-of-concept, fluorescence dequenching was tested with proteinase K (Thermo Scientific, 20 mg/mL) in splicing buffer for 1 h at 25 °C. The maximum fluorescence intensity was set to 100%. As control, the same procedure was performed with the corresponding fluorophore-labeled I^N fragment. For back-correction against N-terminal cleavage, HI^{C(N154A, S+1A)T} was used. Fluorescence dequenching upon *trans*-splicing was performed with 1 μM or 10 nM of F/Q-modified I^N fragment in combination with 4 μM or 40 nM of HI^CT. Spectra recording was done with a FluoroLog (Horiba Yvon) at ex/em = 470/480-650 nm (FAM/Dabcyl) or ex/em = 630/640-750 nm (sCy5/BHQ-3).

Real-time monitoring of *trans*-splicing

1 μM or 10 nM of F/Q-modified I^N were combined with 4 μM or 40 nM of HI^CT in splicing buffer (50 mM Tris, 300 mM NaCl, 1 μM EDTA, 0.1 mM TCEP, 10% glycerol, pH 7.0) in the absence or presence of human cell lysates and fluorescence release was followed over 1 h at 25 °C. Analysis of fluorescence dequenching in real-time was performed on a FluoroLog (Horiba Yvon) at ex/em = 480/520 nm (FAM/Dabcyl) or ex/em = 640/670 nm (sCy5/BHQ-3). For corroborating covalent N-terminal protein labeling, samples were taken after 0, 5, 10, 15, 30, 45, and 60 min of *trans*-splicing and analysed by SDS-PAGE in-gel fluorescence.

Analysis of protein *trans*-splicing kinetics

For determination of $\tau_{1/2}$ values, sequential spectra recording after 0, 1, 2, 3, 5, 10, 15, 20, 30, 45, and 60 min was performed. The maximum fluorescence intensities of the respective spectra were plotted against the reaction time and fitted by non-cooperative (n = 1) Hill equation. The pseudo first-order rate of protein *trans*-splicing was derived from real-time monitoring measurements through data fitting with

$$P = P_0 (1 - e^{-kt}) \quad (\text{Eq. 4})$$

where P is the percentage of splice product formation at time t, P_0 being the splicing yield and k the observed rate.

Solid-phase peptide synthesis and Ni(II) loading

All I^N fragments were synthesized via Fmoc-based SPPS on a Rink amide MBHA resin as a solid support by a Liberty microwave peptide synthesizer (CEM, Kamp-Lintford, Germany) with a standard protocol (54 W, 3 min, 75 °C; 50 °C for cysteine building blocks). The amino acid side-chains were protected as follows: Asp(tBu), Cys(Mmt), Glu(tBu), Lys(Boc), and Ser(tBu). The coupling reactions with the Liberty microwave peptide

synthesizer were performed by activating 0.2 M of Fmoc-protected amino acid with 0.5 M of HBTU and HOBT*H₂O in the presence of 2 M DIPEA in NMP. A double coupling for all amino acids was performed. Removal of the Fmoc group was carried out with 20% piperidine in DMF. For peptides with the multivalent chelator head, 1.5 eq. Fmoc-Dap(*tris*NTA-OtBu)-OH,¹ 3.0 eq. COMU, and 6.0 eq. DIPEA (0.5 M in DMF) were pre-activated in DMF for 1 min, then added to the resin and agitated over night at RT.⁴ N-terminal labeling was performed either with FAM or sCy5 NHS directly on the resin. FAM was incorporated at the deprotected N terminus using 5.0 eq. FAM, 4.7 eq. HBTU, and 6.0 eq. NMM (400 mM in DMF). To increase the labeling efficiency, coupling of FAM was performed twice. sCy5 NHS labeling was performed with 1.5 eq. dye, 10 eq. DIPEA in DMF. Afterwards, free primary amines were acetylated with acetic anhydride, DIPEA, and water-free DMF (1.0:0.5:8.5) twice for 15 min. Next, the resin was extensively washed with DMF, DCM, MeOH, and Et₂O and finally dried under vacuum for at least 2 h. The cleavage of the peptides was achieved by an incubation with a cleavage cocktail containing TFA/H₂O/thioanisole/phenol (95:1.25:1.25:1.25) for 1-2 h. Cleaved peptides were precipitated in ice-cold Et₂O, centrifuged, washed with ice-cold Et₂O, dissolved in *t*BuOH/H₂O (4:1), and finally lyophilized. The purification of FAM- and sCy5-labeled peptides was performed by semi-preparative RP-C₁₈ HPLC (PerfectSil C18 column 250 x 22 mm 300 ODS, 5 μ m, MZ Analytical, Mainz, Germany) under acidic conditions (buffer A: 0.05% TFA (aq.); buffer B: MeCN + 0.05% TFA) with 4 mL/min. After peptide confirmation by MALDI-TOF MS, the respective fluorescence quenchers Dabcyl NHS or BHQ-3 NHS were incorporated at the C-terminal lysine by using 1.5 eq. quencher in dry DMSO (final concentration 10% v/v) and 1.0 eq. of fluorophore-labeled peptide in 0.1 M sodium bicarbonate buffer pH 8.3 at 25°C for at least 8 h. After lyophilization, the product was purified by RP-C₁₈ HPLC (PerfectSil C18 column 250 x 10 mm 300 ODS, 5 μ m, MZ Analytical, Mainz, Germany) with detection at 215 nm, 460 nm for FAM/Dabcyl-, or 632 nm for sCy5/BHQ-3-modified peptides. The products were again confirmed by MALDI-TOF MS. For Ni(II) loading, the purified peptides were solubilized in 20 mM HEPES, pH 7.0. Subsequently, a 50-fold excess of NiCl₂ was added and the mixture was incubated for 1 h at 25 °C in the dark. Purification of F/Q-modified I^N-Ni-*tris*NTA was performed by anion exchange chromatography (1 mL HiTrap Q HP, GE Healthcare). After washing with 5 column volumes 50 μ M EDTA in 20 mM HEPES, pH 7.0, the compound was eluted with a gradient starting from 0 to 1 M NaCl in 20 mM HEPES, pH 7.0. Peptide concentrations were determined by UV/Vis spectroscopy (Cary 50 Bio UV/Vis Spectrophotometer, Varian, Palo Alto, USA) at $\lambda = 460$ nm for FAM/Dabcyl ($\epsilon = 108,900$ M⁻¹ cm⁻¹) or at $\lambda = 632$ nm for sCy5/BHQ-3 ($\epsilon = 317,700$ M⁻¹ cm⁻¹).

Tab. S1. RP-C₁₈ HPLC gradients. FAM/Dabcyl-modified peptides were purified with Method 1 and sCy5/BHQ-3-modified peptides with Method 2, respectively.

Method 1		
t (min)	0.05% TFA (aq.) (%)	MeCN + 0.05% TFA (%)
0	95	5
20	0	100
22	0	100
23	95	5
28	95	5

Method 2		
t (min)	0.05% TFA (aq.) (%)	MeCN + 0.05% TFA (%)
0	70	30
30	0	100
32	0	100
33	70	30
38	70	30

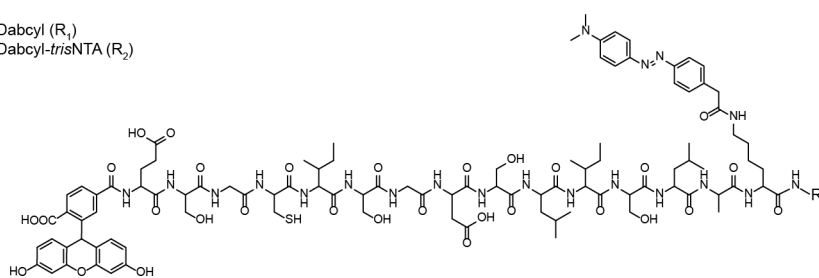
Tab. S2. Calculated and observed molecular weights of synthetic I^N fragments. Molecular weights were determined by MALDI-TOF MS (positive mode).

Compound	Formula	MW _{calc} (Da)	MW _{obs} (Da)
FAM-I ^N -Dabcyl	C ₉₇ H ₁₃₂ N ₂₀ O ₃₀ S	2088.9	2086.5
FAM-I ^N -Dabcyl- <i>tris</i> NTA	C ₁₄₁ H ₁₉₇ N ₂₉ O ₅₄ S	3192.3	3187.9
Cy5-I ^N -BHQ-3	C ₁₂₅ H ₁₇₄ N ₂₅ O ₃₁ S ₃	2617.2	2617.4
Cy5-I ^N -BHQ-3- <i>tris</i> NTA	C ₁₆₉ H ₂₃₉ N ₃₄ O ₅₅ S ₃	3720.6	3721.3

Tab. S3. Summary of fluorescence increase, splice product formation, affinity, and kinetics. Fluorescence increase (ΔF) and splice product formation (SP) were determined after 1 h of PTS. Equilibrium dissociation constants K_D were determined by MST with HI^{C(N154A, S+1A, H73A)}T. $\tau_{1/2}$ values were derived from fluorescence recovery over time. ΔF , SP formation, and $\tau_{1/2}$ were measured with 1 μ M or 10 nM (grey) of respective I^N.

	I ^N fragment	ΔF (x-fold)	SP (%)	K_D (nM)	$\tau_{1/2}$ (min)
FAM/Dabcyl	I ^N	11	75 \pm 5	425 \pm 35	12 \pm 2
	I ^N - <i>tris</i> NTA	9	65 \pm 5	650 \pm 55	14 \pm 3
	I ^N -Ni- <i>tris</i> NTA	10	70 \pm 4	14 \pm 1	11 \pm 1
		8	61 \pm 8		11 \pm 2
sCy5/BHQ-3	I ^N	13	74 \pm 7	350 \pm 40	12 \pm 2
	I ^N - <i>tris</i> NTA	9	53 \pm 6	600 \pm 50	14 \pm 1
	I ^N -Ni- <i>tris</i> NTA	10	58 \pm 3	29 \pm 10	11 \pm 3
		11	52 \pm 5		11 \pm 3

FAM- I^N -Dabcyl (R_1)
FAM- I^N -Dabcyl-*tris*NTA (R_2)



sCy5- I^N -BHQ-3 (R_1)
sCy5- I^N -BHQ-3-*tris*NTA (R_2)

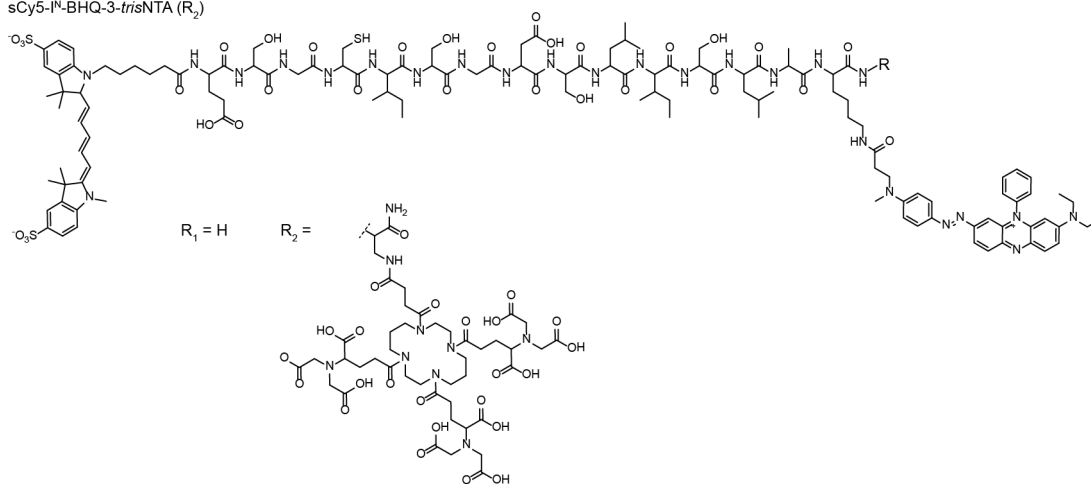


Fig. S1. Chemical structures of synthetic I^N fragments.

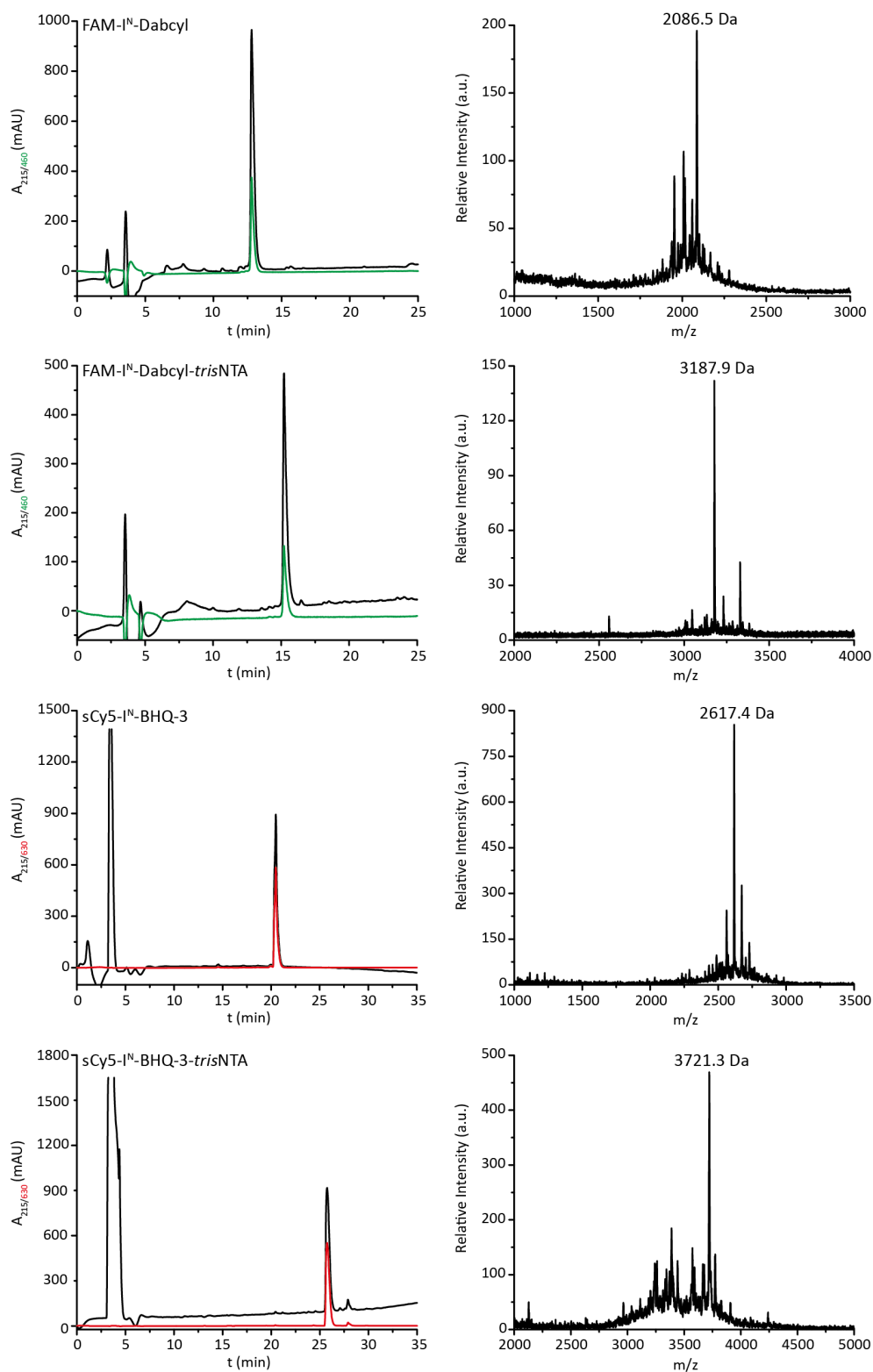


Fig. S2. Analytical RP-C₁₈ HPLC of synthetic I^N fragments and MALDI-TOF MS analysis. Purification and analysis of FAM/Dabcyl-modified I^N fragments (Method 1) and sCy5/BHQ-3-modified I^N fragments (Method 2) were performed with a PerfectSil C18 column 250 x 22 mm 300 ODS, 5 μm (MZ Analytical, Mainz, Germany). Calculated and observed molecular weights of MALDI-TOF MS analysis are summarized in Table S2.

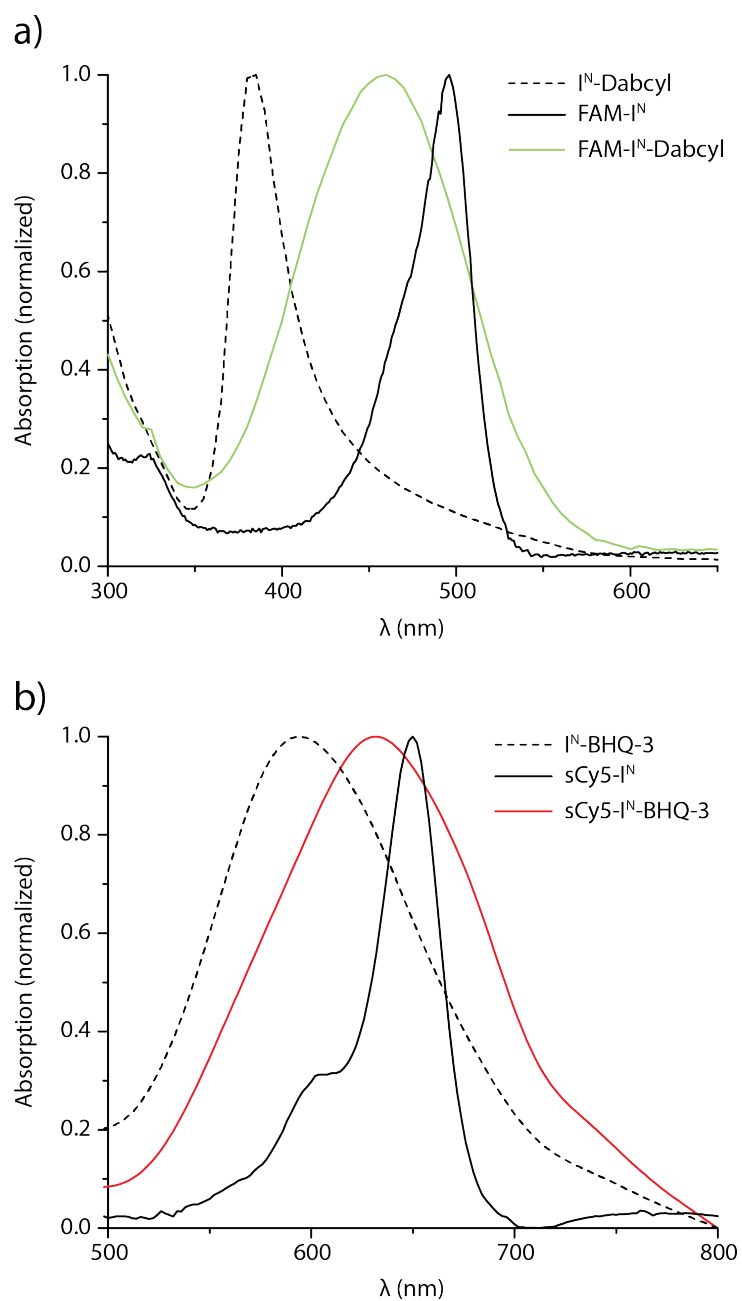


Fig. S3. UV/Vis spectroscopy of F/Q-modified I^N . (a) FAM- I^N -Dabcyl showed $\lambda_{\max} = 460$ nm, whereas I^N -Dabcyl and FAM- I^N displayed $\lambda_{\max} = 384$ nm and $\lambda_{\max} = 495$ nm, respectively. (b) Broad absorption of sCy5- I^N -BHQ-3 with $\lambda_{\max} = 632$ nm was recorded. A different absorption was perceived for I^N -BHQ-3 with $\lambda_{\max} = 595$ nm and for sCy5- I^N with $\lambda_{\max} = 650$ nm.

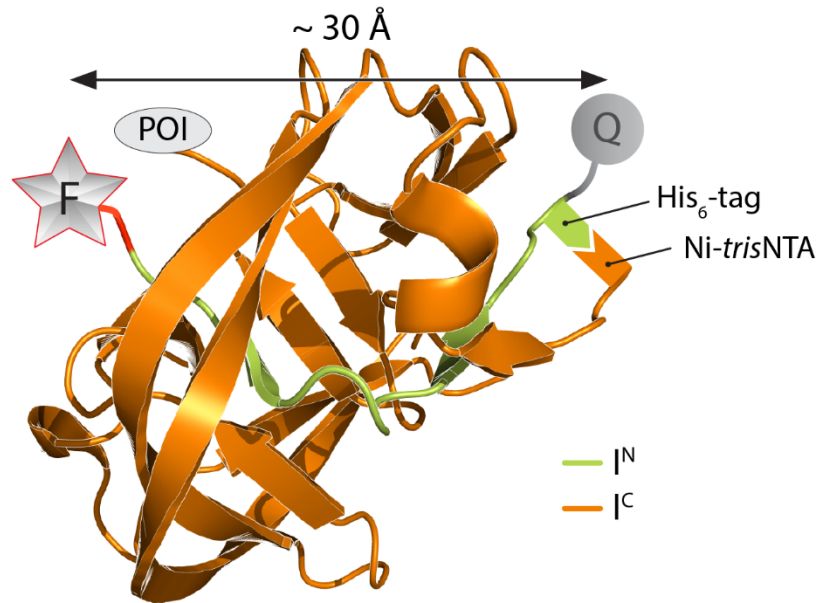


Fig. S4. Distance estimation between fluorophore and quencher. The crystal structure of the *Ssp* Dna mini-intein (1MI8.pdb) in the pre-splicing state was used for distance estimation between fluorophore (F) and quencher (Q) of I^N (light orange). Herein, an optimal distance for fluorescence quenching of ~30 Å was determined. The recombinant I^C is shown in dark orange. Distance estimation was performed with PyMol software package.

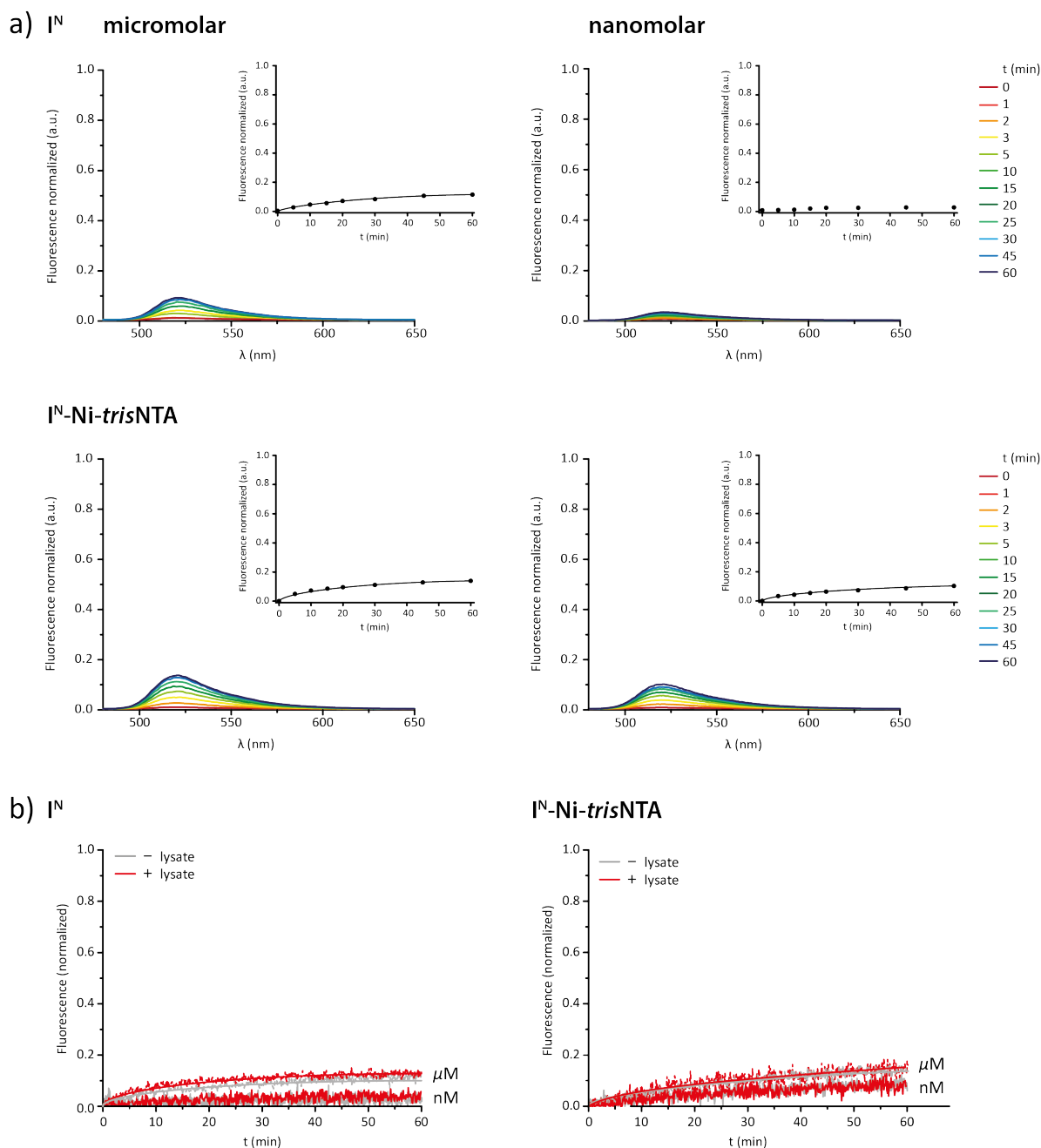


Fig. S5. N-terminal cleavage of I^N fragments. (a) Fluorescence increase of 1 μ M/10 nM of FAM- I^N -Dabcyl with 4 μ M/40 nM of $HI^{C(N154A, S1+A)}_T$ due to N-terminal cleavage of I^N was monitored at RT. Fluorescence spectra were sequentially recorded after 0, 5, 10, 15, 20, 30, 45, and 60 min, illustrated in rainbow color. At μ M concentrations, $9 \pm 2\%$ fluorescence dequenching was observed, whereas no significant dequenching could be observed in the nanomolar range. Using 1 μ M/10 nM of FAM- I^N -Dabcyl-Ni-*tris*NTA, $13 \pm 1\%$ (μ M) and $10 \pm 1\%$ (nM) fluorescence release upon N-terminal cleavage was detected. (b) Fluorescence release over 1 h at RT with 1 μ M/10 nM of sCy5- I^N -BHQ-3 as well as sCy5- I^N -BHQ-3-Ni-*tris*NTA with 4 μ M/40 nM of $HI^{C(N154A, S1+A)}_T$ was followed in the absence and presence of human cell lysates. At μ M concentrations, $9 \pm 3\%$ (I^N) and $14 \pm 2\%$ (I^N -Ni-*tris*NTA) fluorescence release was observed, whereas in the nanomolar range fluorescence increase ($9 \pm 2\%$) was only detected with I^N -Ni-*tris*NTA.

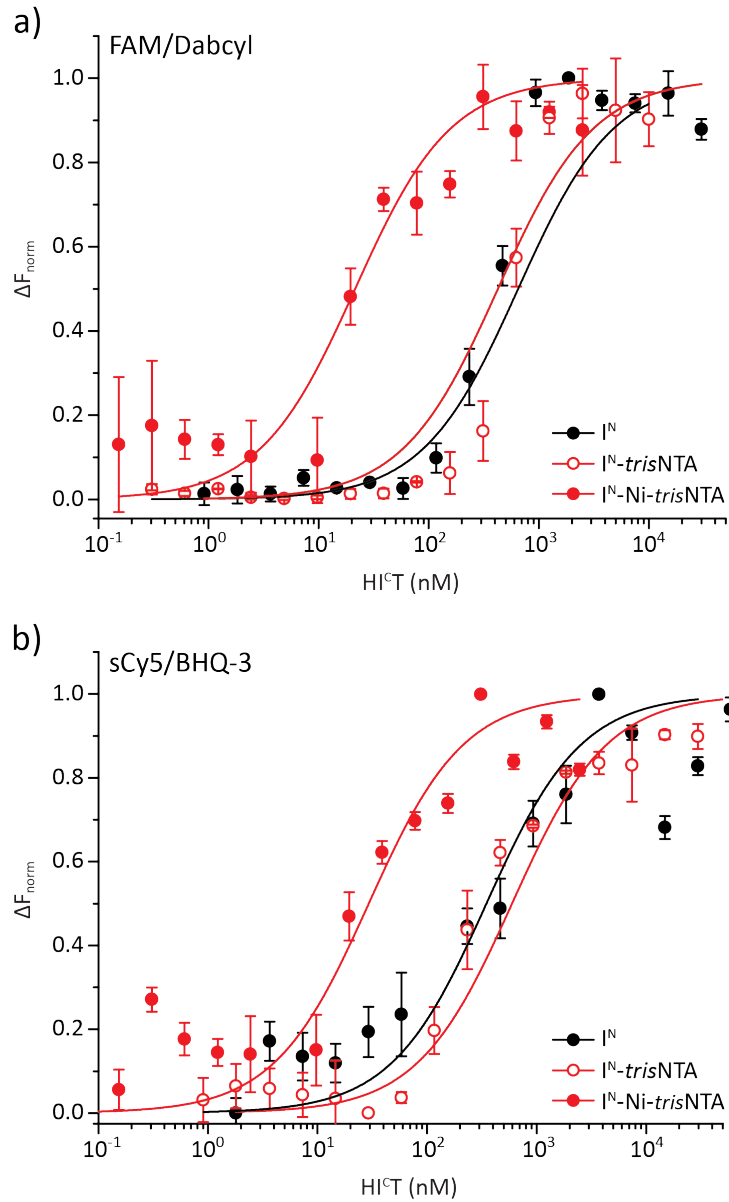


Fig. S6. Microscale thermophoresis analysis of F/Q-modified I^N fragments with HI^{CT}. FAM/Dabcyl (a) as well as sCy5/BHQ-3 (b) modified I^N , I^N -trisNTA, and I^N -Ni-trisNTA (2 nM each) were titrated with different concentrations of splice-inactive HI^{CT} at RT. Changes in fluorescence were normalized (ΔF_{norm}). In the presence of Ni-trisNTA, the affinity of the intein fragments was dramatically increased.

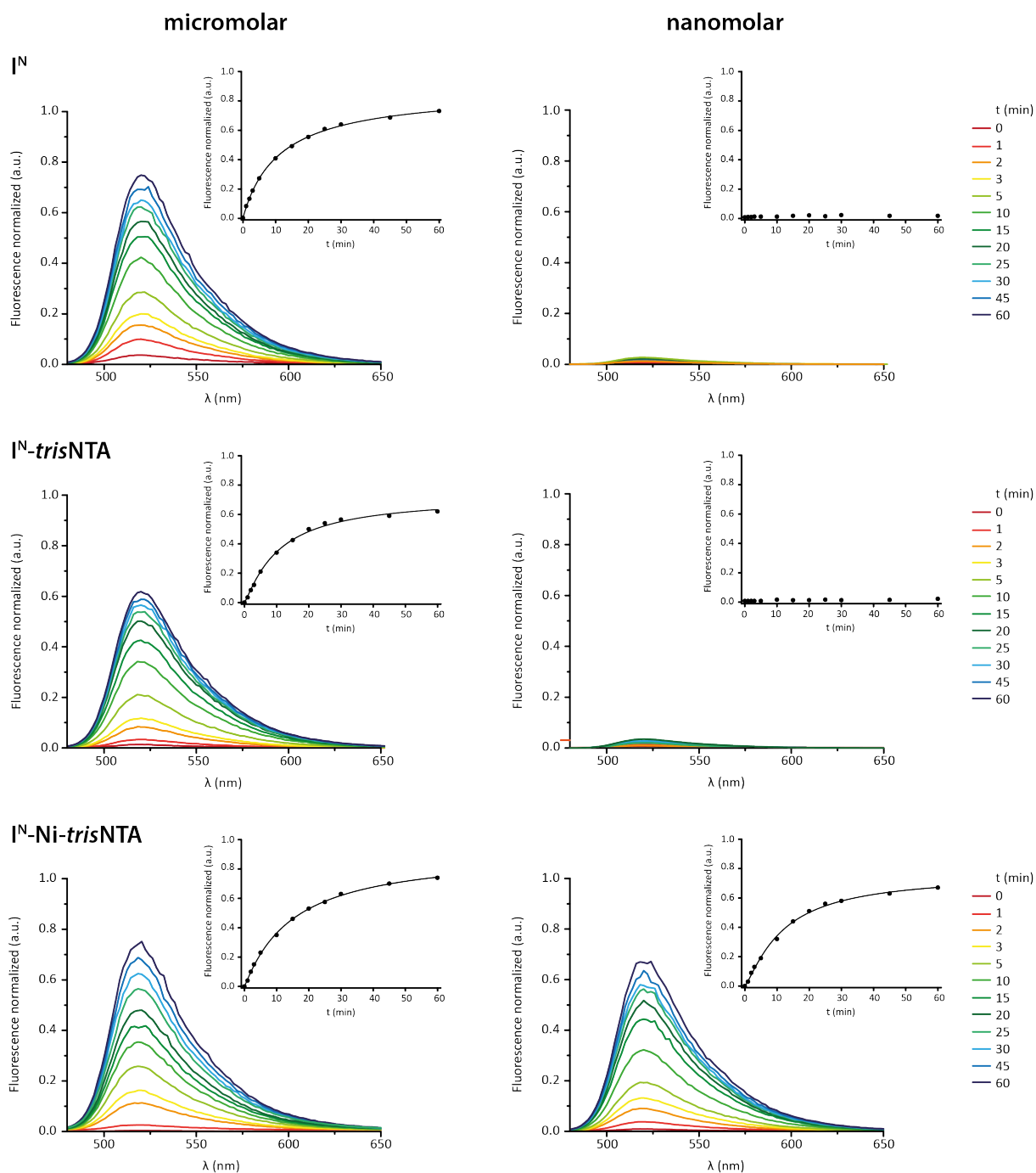


Fig. S7. Fluorescence dequenching and $\tau_{1/2}$ determination of *trans*-splicing. Fluorescence spectra were sequentially recorded after 0, 1, 2, 3, 5, 10, 15, 20, 25, 30, 45, and 60 min of reaction at RT. Increasing reaction times are illustrated in rainbow color. Fluorescence intensities at the peak maxima are plotted against the *trans*-splicing reaction time to obtain $\tau_{1/2}$ values. Efficient fluorescence release could be observed for 1 μM of I^N , I^N -*trisNTA*, and I^N -*Ni-trisNTA* with 4 μM of HI^{CT} . However, when the concentration was decreased by two orders of magnitude (10 nM and 40 nM), fluorescence dequenching was exclusively observed in the presence of the *Ni-trisNTA*/His-tag recognition element. To correct against N-terminal cleavage of F/Q-modified I^N fragments, control experiments were performed with $\text{HI}^{\text{C(N154A, S+1A)}}_{\text{T}}$.

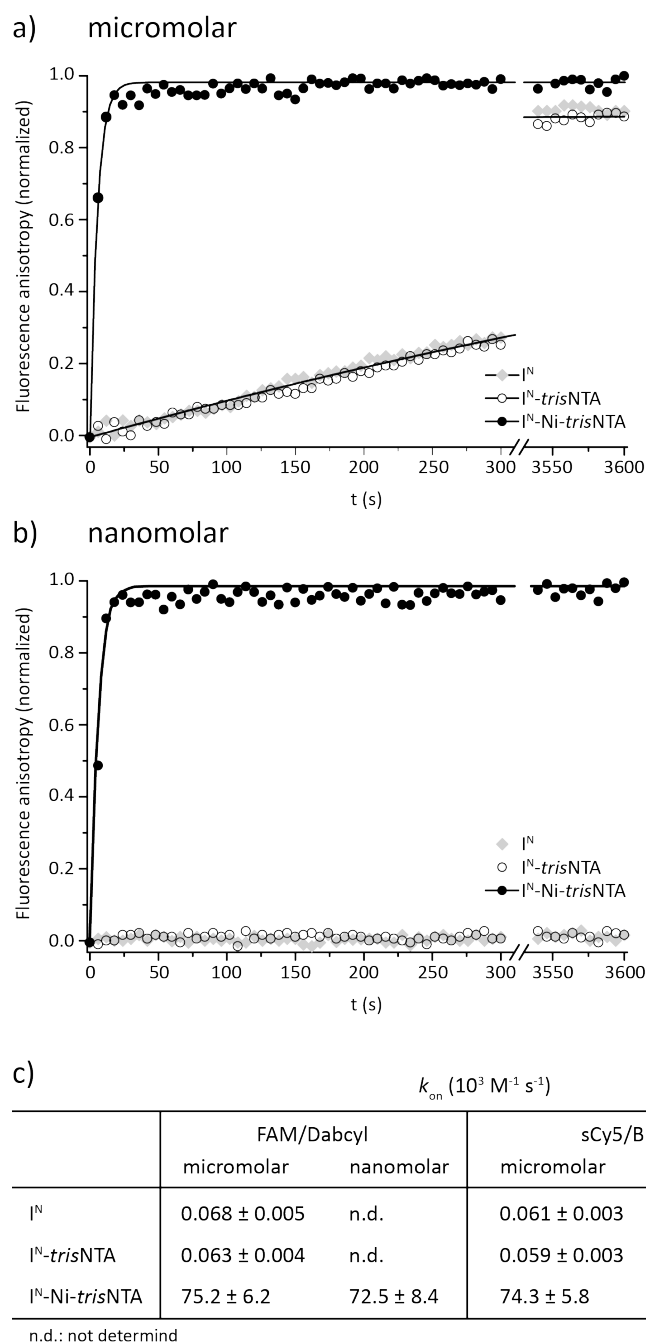


Fig. S8. Fragment association investigated by fluorescence anisotropy. Representative curves for time-dependent increase of fluorescence anisotropy of (a) $1 \mu\text{M}$ of FAM/Dabcyl-modified I^N , I^N -*trisNTA*, and I^N -Ni-*trisNTA* with $4 \mu\text{M}$ of splice-inactive $\text{HI}^{\text{C(N154A, S+1A, H73A)}}_{\text{T}}$ and (b) 10 nM of FAM/Dabcyl-modified I^N , I^N -*trisNTA*, and I^N -Ni-*trisNTA* with 40 nM of splice-inactive $\text{HI}^{\text{C(N154A, S+1A, H73A)}}_{\text{T}}$ were recorded for 1 h at RT. Fluorescence anisotropy is explicitly illustrated from 0-300 s (a, b) to point out the tremendous difference in intein fragment association. c) Association constant k_{on} was determined for both F/Q-pairs at μM and nM concentrations (indicated in a, b) of each intein fragment. In the presence of Ni-*trisNTA*, k_{on} was increased by four orders of magnitude in comparison to I^N in the micromolar range. At nM concentrations, fragment association was exclusively triggered by the high-affinity recognition element.

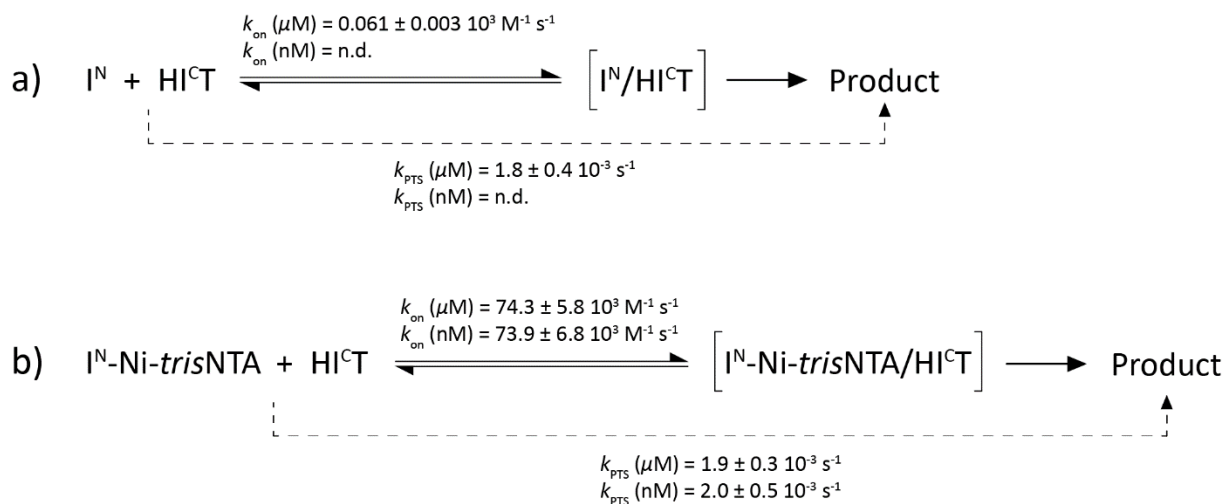


Fig. S9. Reaction kinetics of protein *trans*-splicing. (a) In the absence of the high-affinity recognition element, k_{on} and k_{PTS} values in the μM range were similar to previous literature,⁵ whereas at nM concentrations no fragment association and no PTS were detectable. (b) If *trans*-splicing is triggered by the Ni-*tris*NTA/His-tag interaction, k_{on} values are superimposed by the kinetics of the recognition element, whereas the overall kinetics of PTS (k_{PTS} , dashed arrow) are not influenced. Due to the fact that overall reaction kinetics (k_{PTS}) are very similar in the absence and presence of Ni-*tris*NTA as well as at μM and nM concentrations, the intein fragment association k_{on} is not the rate-limiting step in PTS.

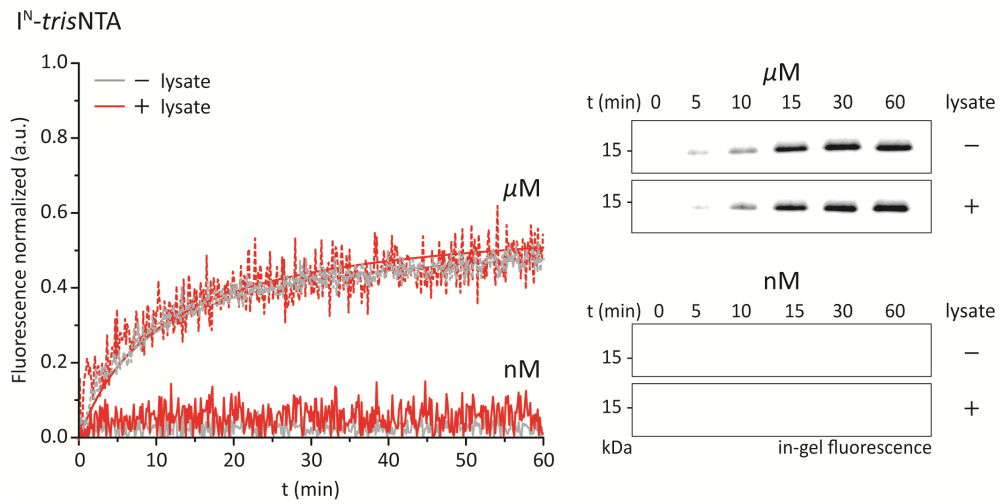


Fig. S10. Real-time monitoring of protein *trans*-splicing. Fluorescence release over 1 h of PTS at RT with either 1 μM /10 nM of sCy5-I^N-BHQ-3-*tris*NTA with 4 μM /40 nM of HI^CT was followed in the absence and presence of human cell lysates. Specific covalent and N-terminal protein labeling with sCy5 was in parallel analyzed by SDS-PAGE in-gel fluorescence at different time points. Correction of fluorescence release due to N-terminal cleavage of sCy5-I^N-BHQ-3-*tris*NTA was performed with HI^{C(N154A, S+1A)}T.

References

- (1) Braner, M.; Kollmannsperger, A.; Wieneke, R.; Tampé, R. *Chem. Sci.* **2016**, *7*, 2646.
- (2) Ludwig, C.; Pfeiff, M.; Linne, U.; Mootz, H. D. *Angew. Chem. Int. Ed.* **2006**, *45*, 5218.
- (3) Seidel, S. A.; Dijkman, P. M.; Lea, W. A.; van den Bogaart, G.; Jerabek-Willemsen, M.; Lazic, A.; Joseph, J. S.; Srinivasan, P.; Baaske, P.; Simeonov, A.; Katritch, I.; Melo, F. A.; Ladbury, J. E.; Schreiber, G.; Watts, A.; Braun, D.; Duhr, S. *Methods* **2013**, *59*, 301.
- (4) El-Faham, A.; Albericio, F. *J. Pept. Sci.* **2010**, *16*, 6.
- (5) Appleby-Tagoe, J. H.; Thiel, I. V.; Wang, Y.; Wang, Y.; Mootz, H. D.; Liu, X. Q. *J. Biol. Chem.* **2011**, *286*, 34440.